

On the Nature of the Jahn-Teller Transition in TiF_3 .

Vasili Perebeinos and Tom Vogt

Department of Physics, Brookhaven National Laboratory, Upton, New York 1973-5000

(Dated: February 7, 2020)

We use first principles density functional theory to calculate electronic and magnetic properties of TiF_3 using the full potential linearized augmented plane wave method. The LDA approximation predicts a fully saturated ferromagnetic metal and finds degenerate energy minima for high and low symmetry structures. The experimentally observed Jahn-Teller phase transition at $T_c=370\text{K}$ can not be driven by the electron-phonon interaction alone, which is usually described accurately by LDA. Electron correlations beyond LDA are essential to lift the degeneracy of the singly occupied $\text{Ti } t_{2g}$ orbital. The LDA+U functional predicts an antiferromagnetic insulator with a orbitally ordered ground state. The input parameters $U=8.1\text{ eV}$ and $J=0.9\text{ eV}$ for the $\text{Ti } 3d$ orbital were found by varying the total charge on the TiF_6^{2-} ion using the molecular NRMOL code. We estimate the Heisenberg exchange constant for spin-1/2 on a cubic lattice to be approximately 24 K. The symmetry lowering energy in LDA+U is about 900 K per TiF_3 formula unit.

PACS numbers: 71.15.Mb, 71.15.-m, 71.30.+h, 64.60.-i

I. INTRODUCTION

There is an ongoing interest in phase transitions in perovskite based materials. Above $T_c \approx 370\text{ K}$ the trifluoride TiF_3 has the cubic framework perovskite structure AMX_3 , with no A cations present. Each Ti is at the center of a corner sharing fluorine octahedra MX_6 . At low temperatures the structure becomes rhombohedral. This symmetry lowering can to a first approximation be characterized by a tilting of the rigid MX_6 octahedra about the threefold axis. The nominal valance of the titanium ion is 3+, with one $3d$ electron occupying the triply degenerate t_{2g} orbital in the high temperature phase. TiF_3 is therefore subject to a Jahn-Teller instability. In the distorted structure titanium has a D_{3d} local environment, in which the t_{2g} orbitals are split into an a_{1g} and a doublet e_g orbital.

We use Density Functional Theory (DFT) to investigate the cubic to rhombohedral structural phase transition which has been established by X-ray diffraction [1, 2]. Many trifluoride MF_3 compounds ($\text{M}=\text{Al, Cr, Fe, Ga, In, Ti, V}$) exhibit this structural phase transition [1, 2, 3, 4]. It is believed that the observed transition in TiF_3 is of a ferroelastic nature [1]. In the distorted structure the fluorine atoms acquire a dipole moment due to the asymmetric distribution of the $2p$ electron density. The long range Coulomb interaction of local dipoles favors a distorted structure with nonzero strain. The Local Density Approximation (LDA) also predicts a distorted structure to have a minimum energy in AlF_3 [5]. Unexpectedly, we find the total energies of the high and low temperature phases to be identical within the errors of calculations. The failure of LDA to explain this phase transition is due to the fact that transition metal d electrons are not adequately described by LDA. There are two competing interactions: the long range ferroelastic interaction and the electron kinetic energy of the t_{2g} one third filled band. The ferro-elastic interaction favors a distorted structure, whereas the octahedra tilting re-

duces the hopping integral (t) between the neighboring Ti atoms and increases the kinetic energy. The two effects cancel each other resulting in degenerate minimums in the potential energy surface.

It was realized some time ago that LDA tends to underestimate the Coulomb repulsion of electrons occupying different orbitals of the same d -shell [6]. In particular, this leads to equal occupations of different orbitals of the same manifold and prevents the stabilization of the orbitally ordered solutions. The LDA+U functional, however, generates an orbital dependent potential which favors solutions with broken orbital degeneracy. Furthermore, the broken symmetry solutions in LDA+U predict a band narrowing effect due to the Coulomb repulsion. LDA+U calculations indicate that the low temperature phase has a by about 900K lower energy per TiF_3 than the high temperature phase. The electronic ground state is orbitally ordered in the low temperature phase with one electron occupying the a_g orbital oriented along the rhombohedral direction forming a Heisenberg spin 1/2 lattice coupled antiferromagnetically to its neighbors via a superexchange mechanism.

The LDA+U bandstructure is sensitive to the input parameters (U and J), where U is the on-site repulsive interaction and J is the exchange constant. In principle, values of U and J should follow from the LDA exchange-correlation potential, which describes sufficiently well the on-site Coulomb repulsion of the singly occupied orbital. The value of U depends on the LDA potential and the chemical environment of the atom and has to be evaluated self-consistently for a given atomic structure. The available recipes [6, 7] differ in the estimates of the parameter U . In the original method by Anisimov et. al. [6] hopping matrix elements from a given atom in the supercell were turned off, which allowed for charge variation on a given atom and calculations of a screened Hubbard U . Using Picket's recipe [7] a charge on a given atom is controlled by the applied external potential, and additional screening due to the hybridization of d orbitals

with oxygen states was gained. The latter results in a U 's which are smaller by about 40%. In this work we use the molecular NRLMOL code [9] to calculate U by changing the occupation number of the Ti d orbital of the TiF_6 ion. The kinetic energy is obviously turned off since there is no other Ti for an electron to hop to and since only the first neighboring fluorines mostly contribute to the screening a good estimate for parameters U and J can be readily achieved in the calculations.

The Hund interaction and the electron kinetic energy are realistically described with LDA. The TiF_3 compound is predicted to be a ferromagnetic metal with a fully saturated magnetic moment of $1 \mu_B$ per formula unit. The exchange Hund energy is large and the Stoner criterium is satisfied. The electron-phonon interaction lifts the on site degeneracy of the t_{2g} orbitals and for a sufficiently strong coupling a gap in the spectrum can open. LDA describes realistically the electron-phonon coupling even for strongly correlated materials like the perovskite LaMnO_3 [8]. However, our calculations of the electron-phonon coupling in TiF_3 rule out this mechanism. The t_{2g} orbitals are pointing along the diagonals between the Ti-F bonds, which intuitively suggests a small electron-phonon coupling, contrary to the situation in LaMnO_3 , where e_g orbitals pointing toward oxygens.

II. METHOD OF CALCULATION

The purpose of this paper is to elucidate the electronic structure of TiF_3 and explain the structural phase transition using the DFT method. This is done using the general potential linearized augmented plane wave (FP-LAPW) method [10] with local orbital extensions [11] in the WIEN2k implementation [12]. The LDA Perdew Wang [13] exchange-correlation potential was used. Well converged basis sets and Brillouin zone sampling were employed. The crystal structure was reported by Kennedy and Vogt [2]. It is cubic at high temperature with a unit cell volume 58.8 \AA^3 . A rhombohedrally distorted structure of the space group $R-3c$ can be characterized by three parameters: (1) volume 56.5 \AA^3 , (2) the octahedra tilt $\alpha = 13^\circ$, and (3) a $c/a = 1.0315$ ratio, which measures the distortion along the rhombohedral direction. There are two titanium and 6 fluorine atoms in the rhombohedral unit cell. The fluorine ions are sitting in the $6e$ sites $((x, -x + 1/2, 1/4), \text{etc.})$, and $\delta = x - 0.75$ is the deviation from cubic positions. The octahedra tilting angle is related to δ by $\tan(\alpha) = 2\sqrt{2}\delta$. The calculations for the high and low symmetry phases were performed using a two formula unit cell and the same k-point mesh, with 292 special k-points in the irreducible Brillouin zone. A tetrahedron method was used for integration over the Brillouin zone.

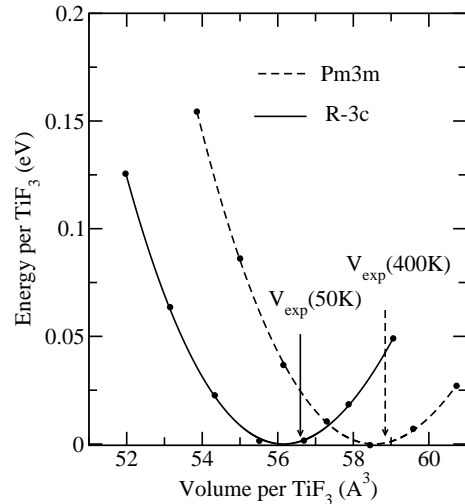


FIG. 1: Calculated total energy of ferromagnetic high-T phase Pm3m (dashed line) and low-T phase R-3c (solid line) as a function of volume. In the low-T phase the ratio c/a was fixed at the experimental value of 1.0315 and the tilt angle at 10° [2].

III. LDA RESULTS

We first assume a cubic symmetry by fixing $\alpha = 0$ and $c/a = 1$. LDA finds a ferromagnetic ground state solution with a fully saturated magnetic moment of $1 \mu_B$ per Ti. The volume optimization is shown in Fig. 1. The equilibrium volume $V_0 = 58.6 \text{ \AA}^3$ is in excellent agreement with the experiment [2]. The bulk modulus of 111 GPa is extracted by fitting a Murnaghan [14] equation of state. The c/a ratio was fixed to the experimental value 1.0315 and the two parameters are relaxed to find the minimum of the low symmetry structure. The energy minimization with respect to the volume for the fixed $c/a=1.0315$ and $\alpha = 10^\circ$ is shown on Fig. 1 and yields $V_m = 56.2 \text{ \AA}^3$.

Further optimization with respect to the tilt angle for a fixed minimum volume V_m and the same c/a ratio did not significantly alter the ground state energy. The optimal tilt angle is $\phi_0 = 10.5^\circ$. The Ti-F bond is the most rigid bond in the structure, and therefore it is convenient to plot the energy versus the Ti-F bondlength. A parabola fit to the energy variation shown on Fig. 2 is excellent and yields a spring constant of the single bond $K = 13.9 \text{ eV}/\text{\AA}$. The Ti-F bond length d in $R3c$ crystal structure is

$$d^2 = a_h^2(1/12 + \delta^2 + (c/a)^2/24) \quad (1)$$

where $a_h = a\sqrt{2}$ is the hexagonal a lattice constant. Knowing the spring constant for the bond stretching and equilibrium volume V_0 the bulk modulus can be estimated as $B = K/(6V^{1/3}) \approx 96 \text{ GPa}$.

The total energy differences of the high- and low-T phases is beyond the accuracy of calculations. Despite the excellent agreement with the experimental structural

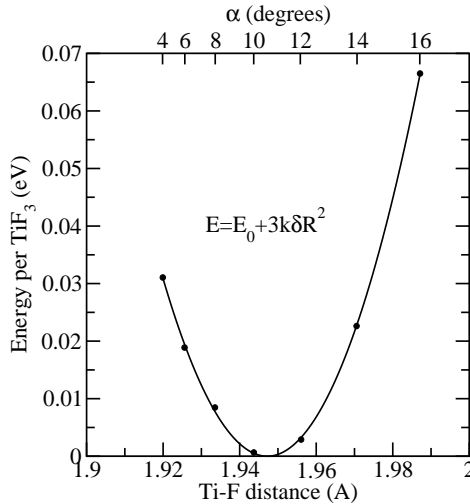


FIG. 2: Calculated total energy of ferromagnetic low-T phase R-3c as a function of the tilt angle and fixed volume and c/a ratio. The optimal Ti-F distance is 1.947 Å and the spring constant is 13.9 eV/Å².

parameters, the LDA total energy analysis does not explain the high temperature of the observed structural phase transition.

The densities of states are shown on Fig. 3. The t_{2g} band lies at the Fermi level and it is one third filled. The Hund energy dominates the kinetic energy such that the Stoner criterium is satisfied and the material becomes magnetic. The band structure of the Ti t_{2g} electrons can easily be understood with a nearest-neighbor two-center Slater-Koster [16] model. The orbitals $|\alpha\beta\rangle$ have hopping matrix elements with themselves along the α and β directions with amplitude $t = (dd\pi)$. The tight binding fit in the high temperature phase with $t = 0.25$ eV is shown on Fig. 4.

In the low temperature phase the Ti-F-Ti bond angle is smaller than 180°, which reduces the hopping and narrows the band width. The onsite orbital degeneracy is lifted by the octahedra tilting. In the D_{3d} local Ti site symmetry the t_{2g} manifold splits into:

$$\begin{aligned} a_g &= \frac{|xy\rangle + |yz\rangle + |zx\rangle}{\sqrt{3}} \\ e_{g1} &= \frac{|yz\rangle - |zx\rangle}{\sqrt{2}} \\ e_{g2} &= \frac{2|xy\rangle - |yz\rangle - |zx\rangle}{\sqrt{6}} \end{aligned} \quad (2)$$

The bandwidth in the tilted structure $\phi = \phi_0$ corresponds to $t = 0.225$ eV and the electron-phonon Jahn-Teller energy gap at Γ point is 6 meV. From the simple tight binding model with these parameters the kinetic energy loss due to the band narrowing effect is 18 meV and it is not even compensated by the lifting of the orbital degeneracy. The total LDA energy includes the lattice

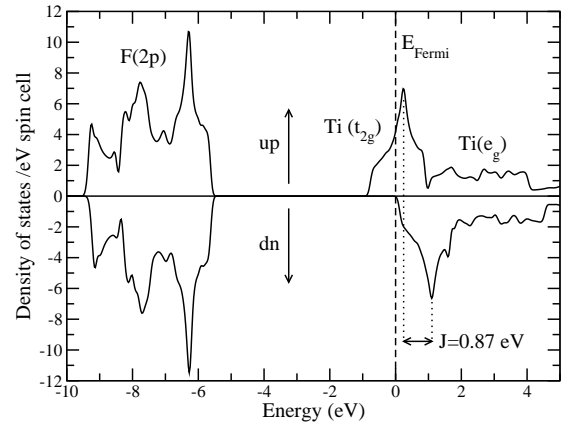


FIG. 3: Density of states of the ferromagnetic solution for $P-mmm$ crystal structure. The t_{2g} and e_g bands are split by the crystal field energy ≈ 2 eV. The t_{2g} bandwidth is about 2 eV, which corresponds to hopping parameter $t = 0.25$ eV. The Hund coupling $J = 0.87$ eV can be estimated from the relative position of the spin up and spin down peak positions.

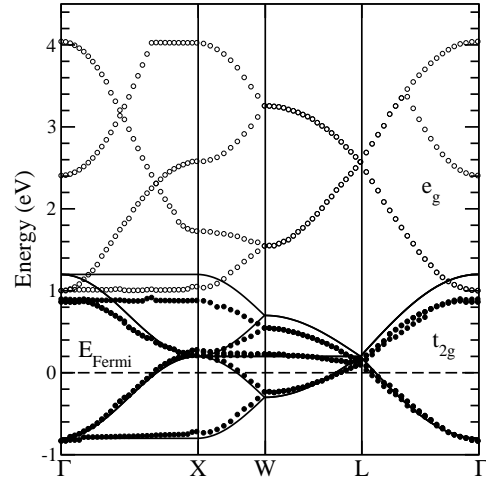


FIG. 4: Calculated band structure along the high symmetry line in the high symmetry structure: e_g bands open circles, t_{2g} bands closed circles. The solid line is a tight binding fit, which uses a single Slater-Koster parameter $t = (dd\pi) = 0.25$ eV. Fermi level is at zero energy.

and electronic degrees of freedom and predicts degenerate minimums within the errors of calculations (Fig. 1). The LDA failure to predict the cubic-to-rhombohedral phase transition can be rationalized by the lack of electron correlation effects in the LDA method.

IV. PARAMETER U (J) CALCULATION FOR LDA+U METHOD

In extending the LDA method to account for correlations resulting from on-site interactions Anisimov, Zaanen, and Andersen (AZA) [6] chose to refine LDA by including an orbital-dependent one-electron potential to

account explicitly for the important Coulomb repulsions not treated adequately in the LDA approach. This was accomplished in accordance with Hartree-Fock theory by correcting the mean-field contribution of the $d-d$ on-site interaction with an intra-atomic correction. This correction has been applied in slightly different ways. We use the SIC LDA+U functional [15] as implemented in the WIEN2k package. LDA+U is no longer a straightforward density functional since it relies on the parameters U and J which depend on the LDA density. To obtain U and J AZA performed LMTO calculations for a supercell in which the d charge on one atom is constrained. The d orbitals on all atoms in the supercell are decoupled entirely from the remaining part of the basis set. This creates a rather artificial system to simulate the screening. To allow hybridization for example, between oxygen p orbitals and d orbitals Pickett, Erwin, and Ethridge (PEE) [7] do not decouple the d states from the surrounding states. PEE employ a generalized constrained density functional approach as proposed by Dederichs et al. [17] to calculate the change in energy due to constraints on local-orbital densities. In a self-consistent calculation, any change in the local orbital charge results in an accompanying change in kinetic energy as well as the potential energy. Since the U term in the LDA+U is a potential energy term, the kinetic-energy change in the constrained LDA calculations should be removed. The contribution to U from the kinetic energy is still an unresolved problem. Values of total U using PEE approach were found to be only 40-65% of the values of Anisimov and co-workers.

In this work we propose to use a single TiF_6^{2-} ion to calculate parameters U and J . The TiF_6^{2-} ion forms an octahedra with a Ti-F bond of 1.93 Å with the Ti atom placed in the center. The total energy and d orbital chemical potential of the TiF_6 can be modeled by the single site Hubbard model:

$$\begin{aligned} E &= E_0 - \varepsilon(n_\uparrow + n_\downarrow) + \frac{U}{2}(n_\uparrow + n_\downarrow)^2 - \frac{J}{2}(n_\uparrow^2 + n_\downarrow^2) \\ \mu_\uparrow &= \frac{\partial E}{\partial n_\uparrow} = -\varepsilon + U(n_\uparrow + n_\downarrow) - Jn_\uparrow \\ \mu_\downarrow &= \frac{\partial E}{\partial n_\downarrow} = -\varepsilon + U(n_\uparrow + n_\downarrow) - Jn_\downarrow, \end{aligned} \quad (3)$$

where n_\uparrow and n_\downarrow are occupation numbers of the triply degenerate t_{2g} molecular orbital. In these calculations the screening due to the nearest neighboring fluorines is taken into account. There are no other Ti atoms for the d electron to hop to. We use two sets of self-consistent calculations to determine the parameters U and J . The nonmagnetic $n_\uparrow = n_\downarrow = n/2$ calculations are shown in Fig. (5,a). The quadratic total energy and linear chemical potential fits give $U_1^{\text{eff}} = U - J/2 = 7.66$ eV. From the magnetic calculation $n_\uparrow = n$, $n_\downarrow = 0$ shown in Fig. (5,b) the quadratic energy and linear μ_\uparrow fit we find $U_2^{\text{eff}} = U - J = 7.24$ eV, such that $U = 8.08$ eV and $J = 0.84$ eV. The linear fit for μ_\downarrow shown in Fig. (5,b)

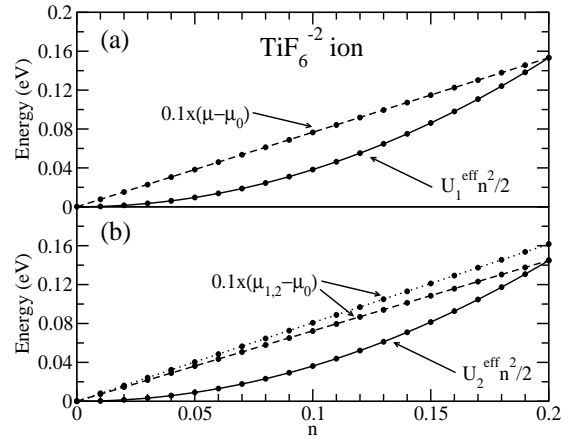


FIG. 5: Calculations of the parameters U and J using TiF_6^{2-} ion (a) paramagnetic calculations (b) magnetic calculations. The solid line is quadratic contribution to the total energy after subtracting linear term. The dashed line is the t_{2g} orbital eigenvalue for spin up electrons scaled by 0.1 and dotted line is spin down t_{2g} orbital eigenvalue. All five curves are fitted by Eq. 3 with parameters $U = 8.08$ eV and $J = 0.84$ eV.

yields the same value of $U = 8.08$ eV. The Hund coupling parameter J should be compared with the spin up and down energy bands splitting in ferromagnetic LDA calculations Fig. 3, which is $J = 0.87$ eV.

The ionic calculations gives the upper boundary for the Coulomb repulsion, because only electrons on the nearest neighbors were allowed to participate in screening. However, we believe the major screening contribution is given by the nearest atoms. We would like to make a comment on the kinetic energy LDA contribution to parameter U . Although, the titanium d orbital can not delocalize on to other Ti atoms, the self-consistent kinetic energy contribution to the total energy also has a quadratic contribution to the total energy. It contributes -1.8 eV and -0.7 eV to U_1^{eff} and U_2^{eff} respectively. If one tries to estimate the parameters U and J using only the potential energy contribution to the effective $U_{1,2}^{\text{eff}}$ one gets an unreasonably large value of $J = 3$ eV. The same unrealistic result was obtain by Pickett et. al. [7]. This indicates that it is very problematic to assign a physical meaning to separate contributions in the LDA potential other than total energy, eigenvalues and electron density.

Usually in oxides the parameter U is estimated to be small. In YTiO_3 Sawada and Terakura [18] estimate $U - J = 3.2$ eV, from analysis of optical data of Okimoto et al. [19] uses $U = 4$ eV. The fluorine potential bounds p electrons stronger than an oxygen potential. Therefore fluorine electrons are less free to contribute to screening of the d titanium orbital. We used a single molecule of YTiO_3 to estimate $U_1^{\text{eff}} = 4.3$ eV from nonmagnetic calculations. The Ti atom was placed at the center and the three oxygens along the x , y , and z directions and a Y atom along the (111) directions. The Ti-O and Ti-Y distances are 2.05 Å and 3.35 Å respectively. As expected

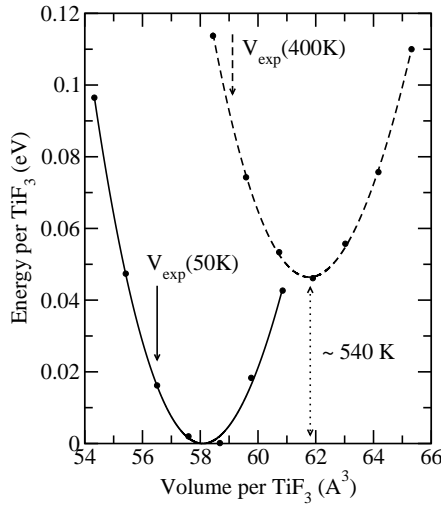


FIG. 6: LDA+U calculations of the antiferromagnetic high-T phase Pm3m (dashed line) and low-T phase R-3c (solid line) as a function of the volume of TiF_3 . Coulomb and exchange parameters were chosen $U=8.1$ eV and $J=0.9$ eV. In the low-T phase the ratio c/a was fixed at experimental values 1.0315 and internal parameter tilt angle at $\phi = 12^\circ$. The optimal volumes of 61.8 \AA^3 and 58.1 \AA^3 agrees well with experimental results indicated by arrows.

the ionic calculations overestimate the parameter U by about 20% with respect to the empirical values. The Ti ion in YTiO_3 molecule has only three oxygen neighbors where as in real crystal there are six. The calculation for the TiF_3 molecule with three neighboring fluorine at the same distances as in the TiF_6^{2-} calculations yielded $U_1^{eff} = 8.73$ eV, which is 14 % larger. This suggests to us that the parameters $U = 8.1$ eV and $J = 0.9$ eV are realistic for TiF_3 and will therefore be used in the next section.

V. LDA+U RESULTS

The volume optimization of the high symmetry phase gives $V_0 = 61.8 \text{ \AA}^3$ and the bulk modulus extracted from the Murnaghan fit shown on Fig. 6 is 110 GPa. The electron correlations on the Ti d orbitals reduces the bandwidth ($4t/U$), such that the kinetic energy variation with respect to the lattice constant is smaller in the LDA+U functional resulting in a larger equilibrium lattice constant compared to the LDA result.

The low symmetry optimization was first done with respect to volume for a fixed experimental tilt angle $\phi = 12^\circ$ and the ratio $c/a = 1.0316$. The optimal volume is 58.1 \AA^3 . Further optimization with respect to the tilt angle for the fixed equilibrium volume gives an additional energy gain of 130 K per Ti such that the distorted structure with the optimal tilt angle of 14° is lower in energy by 675 K per Ti. The parabola fit to the Ti-F bond length variation shown on Fig. 7 gives

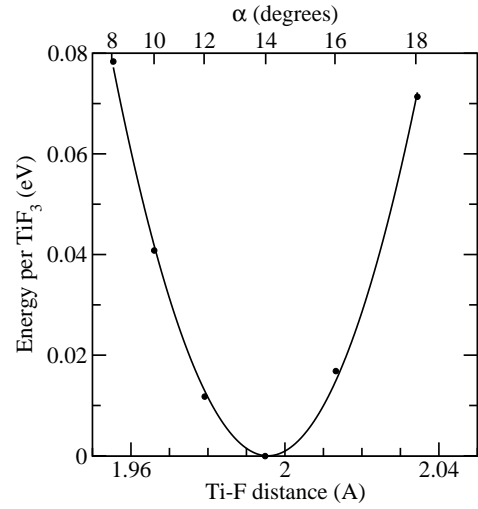


FIG. 7: LDA+U calculations for the antiferromagnetic low-T phase R-3c as a function of the tilt angle and fixed volume V_m and c/a ratio. The optimal angle is 14.1° , which corresponds to Ti-F distance 1.996 \AA . The spring constant is $15.95 \text{ eV}/\text{\AA}^2$.

spring constant $K = 15.95 \text{ eV}/\text{\AA}^2$, The corresponding bulk modulus $B = K/(6V^{1/3}) \approx 108 \text{ GPa}$ is an in excellent agreement with Murnaghan fit Fig. 6.

The density of states for the distorted structure is shown on Fig. 8. The fluorine $2p$ states are not much affected by the correlations. Whereas dramatic differences are seen for the Ti d states. First, LDA+U predicts a gap in the t_{2g} band, which is split into three distinct narrow peaks originated from the a_g and two e_g orbitals. The lowest energy a_g orbital is fully occupied with a spin up electron on one atom and a spin down on the other atom coupled antiferromagnetically. The electronic properties of TiF_3 can be described by the Hubbard Hamiltonian:

$$\begin{aligned} \mathcal{H}_{\text{el}} = & \sum_{i,\alpha\beta,\sigma} -t \left(c_{\alpha\beta,\sigma,i}^\dagger c_{\alpha\beta,\sigma,i+\alpha} + c_{\alpha\beta,\sigma,i}^\dagger c_{\alpha\beta,\sigma,i+\beta} \right) \\ & + \sum_{i,\alpha\beta,\sigma} \frac{U}{2} (n_{\alpha\beta,\sigma,i} n_{\alpha\beta,-\sigma,i}) \\ & + \sum_{i,\alpha\beta \neq \alpha'\beta',\sigma,\sigma'} \frac{U' - J\delta_{\sigma,\sigma'}}{2} (n_{\alpha\beta,\sigma,i} n_{\alpha'\beta',\sigma',i}) \end{aligned} \quad (4)$$

The first term is a kinetic energy term described in Section III. To place two electrons with opposite spins costs energy U , if they occupy the same orbital, or U' , if they are on different orbitals. If the spins of two electrons on different orbitals are aligned the energy cost is reduced by J . In the atomic limit the relation $U = U' + 2J$ holds. The second order perturbation theory of the Hamiltonian (Eq. 4) with respect to t/U predicts an insulating antiferromagnetic ground state solution for parameters $U = 8.1$ eV, $J = 0.9$ eV and $t = 0.22$ eV.

The superexchange energies per Ti of the antiferromagnetic Neel state and ferromagnetic solutions, with a_g

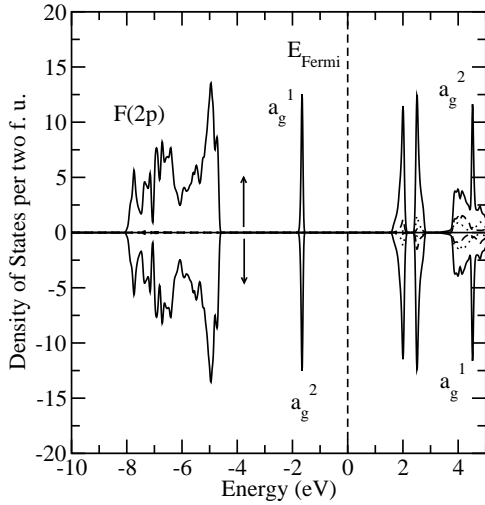


FIG. 8: Density of States per two formula units per eV. The two electrons in the unit cell fill the a_g^1 spin up orbital on atom one and the a_g^2 spin down orbital on the second atom peaked at -1.64 eV. The two lowest unoccupied peaks (at 2.01 eV and 2.52 eV) are due to the e_g orbitals of the t_{2g} manifold. The lower energy orbital is due to the e_g orbital of the same atom and spin as the occupied a_g orbital. The broad bands 2 eV higher in energy shown by the dashed and dotted lines are due to the $e_g = \{x^2 - y^2, 3z^2 - r^2\}$ orbitals split by crystal field. The empty a_g orbital with opposite spin at 4.53 eV forms a resonance in the crystal field e_g background.

orbital Eq. 2 occupied in both cases, are:

$$E_{\text{AFM}} = -\frac{4t^2}{3} \frac{1}{U'} - \frac{8t^2}{3} \frac{1}{U}$$

$$E_{\text{FM}} = -\frac{4t^2}{3} \frac{1}{U' - J} \quad (5)$$

where the first term is due to virtual hopping of the localized electron on the six neighboring e_g orbitals. The second term in E_{AFM} is due to virtual hopping of the a_g orbital to the 6 neighbors with the hopping amplitude $2t/3$, and it is missing in the ferromagnetic ground state due to the Pauli principle. The $LDA + U$ energy differences between the ferromagnetic and antiferromagnetic ground states and the fixed optimal distorted geometry are shown on Fig. 9. Both the perturbation theory and the $LDA + U$ results predict the antiferromagnetic to ferromagnetic transition at $U/J \approx 4$. For the large U/J values $LDA + U$ underestimates the exchange energy by a factor of 2 and for the realistic parameter of $U = 8.1$ eV it predicts an energy difference of 72 K between the two phases. Neglecting the zero-point energy of the spin waves the energy difference between the parallel and anti-parallel classical spins on a cubic lattice is $6JS(S + 1)$ [20]. For spin $S = 1/2$ this yields $J = 16$ K and the corresponding Neel temperature in the mean field approximation is $T_N = 1.5J = 24$ K. The quantum fluctuations reduces the Neel temperature to $T_N = 0.946J = 15$ K [21]. However, the neutron diffraction experiment [22]

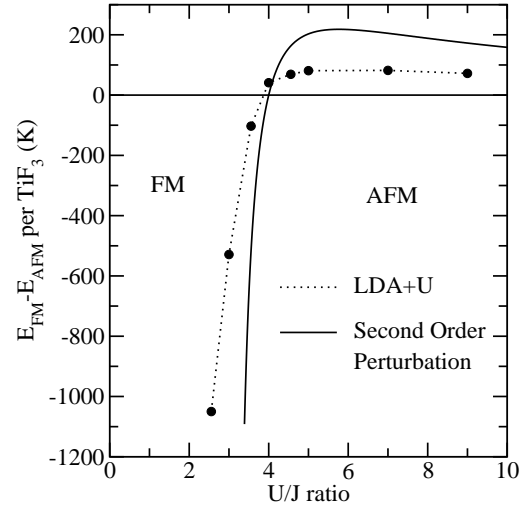


FIG. 9: Energy difference of the total energy of ferromagnetic and antiferromagnetic solutions as a function of U/J ratio. The solid line is a second order perturbation theory for the fixed values $J = 0.9$ eV and $t = 0.225$ eV. The dots are $LDA + U$ results with fixed $J = 0.9$ eV and optimal low temperature geometry.

did not reveal any long range magnetic order down to 10 K. Whether the absence of magnetic long range order in TiF_3 is an intrinsic effect due to the coupling of the orbital and spin degrees of freedom or extrinsic due to the presence of the multidomain structure observed in the low symmetry phase by Mogus-Milankovic et al. [1] requires further theoretical and experimental investigations.

X-ray diffraction measurements under pressure by Sowa and Ahsbahs [23] allow us to determine the experimental bulk modulus of TiF_3 . Fig. 10 (a) shows data points along with Birch-Murnaghan equation of state fit. The fit to the full range of pressures predicts a physically unreasonable small bulk modulus $B = 7.5$ GPa and unphysically large coefficient $K_2 = 142$ GPa $^{-1}$. The first derivative is fixed to $K_1 = 4$ in the Birch-Murnaghan equation of state:

$$P(V) = 3Bf(1 + 2f)^{5/2} \left(1 + \frac{3f^2}{2} \left(BK_2 + \frac{35}{9} \right) \right) \quad (6)$$

where $f = 0.5((V_0/V)^{2/3} - 1)$ and V_0 is the volume at ambient pressure. The high pressure points (above 4 GPa) can be fitted by Eq. (6) to give $B = 51$ GPa and a normal $K_2 = -0.005$ GPa $^{-1}$. However, the volume at normal pressure has to be fixed to $V_0 = 51.9$ Å 3 , which is 11% smaller than the observed one. We speculate that this anomalous behavior of the compressibility of TiF_3 is due to the presence of domain walls in the low symmetry phase observed in [1]. Under applied pressure the crystal becomes a single domain. To check for this assumption we calculate the bulk modulus of the lower symmetry phase using the experimental c/a and V/V_0 ratios [23]. The tilt angle was chosen to keep the Ti-F

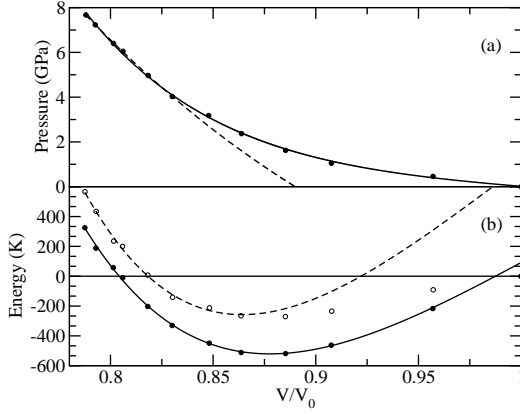


FIG. 10: (a) experimental P – V diagram fitted by the Birch-Murnaghan equation of state to all data points (solid line) and the first six high pressure points (dashed line). (b) bulk modulus calculations using the cell parameters given in table I. Energies of LDA (LDA+U) calculations are shown by open (filled) circles. The Birch-Murnaghan fit to the high pressure points is shown by the dashed (solid) line for LDA (LDA+U) calculations. The zero energy is chosen at the ambient pressure value.

bondlength Eq. (1) constant for all pressure values. We fix $d_{Ti-F} = 1.947 \text{ \AA}$ and $d_{Ti-F} = 1.996 \text{ \AA}$ for LDA and LDA+U calculations respectively. For LDA+U calculations V_0 was fixed to the experimental value [23] $V_0 = 58.3 \text{ \AA}^3$, while for LDA it is reduced to match the optimal volume $V_0 = 56.2 \text{ \AA}^3$ to eliminate the strain effects. The results of calculations for the unit cell parameters given in table I are shown on Fig. 10 (b). The high pressure points can be fitted by Eq. (6) to give a bulk modulus of $B = 42 \text{ GPa}$ for LDA and $B = 29 \text{ GPa}$ for LDA+U functionals with corresponding coefficients $K_2 = -0.011 \text{ GPa}^{-1}$ and $K_2 = -0.008 \text{ GPa}^{-1}$ and optimal volumes $V/V_0 = 0.86$ and $V/V_0 = 0.88$. The energies in the global minimums in LDA and LDA+U calculations are 270 K and 525 K per TiF_3 lower than that of the experimentally observed structural parameters. A shallower minimum in LDA can be explained by the kinetic energy loss due to the octahedra tilting. In LDA+U the kinetic energy is suppressed due to correlations and does not change much with tilting. An alternative explanation of the anomalous behavior of the compressibility can be attributed to the phonon contribution to the free energy which in principle depends on pressure. Additional theoretical calculations of the phonon spectrum and its pressure dependence (Gruneisen parameter) is needed to estimate the phonon contribution to the bulk modulus anomaly.

VI. CONCLUSION

We used density functional theory to predict the electronic and magnetic properties of TiF_3 . LDA predicts TiF_3 to be a ferromagnetic metal with a fully saturated moment $1 \mu_B$ per Ti. The energies of the high and the

TABLE I: The unit cell parameters for the bulk modulus calculations. The normalized volume V/V_0 and c/a ratios are taken from Sowa and Ahsbahs [23]. For LDA+U calculations we used experimental volume $V_0 = 58.3 \text{ \AA}^3$ at ambient pressure [23] and we choose a smaller $V_0 = 56.2 \text{ \AA}^3$ for LDA calculations to match the LDA optimal value. For given volume and c/a ratios the tilt angle was chosen such as Ti-F bondlength Eq. (1) is constant and equal to $d_{Ti-F} = 1.947 \text{ \AA}$ and $d_{Ti-F} = 1.996 \text{ \AA}$ for LDA and LDA+U respectively.

p (GPa)	V/V_0	c/a	α^0 LDA	α^0 LDA+U
0.0001	1.000	1.023	10.4	13.9
0.46	0.957	1.056	14.3	17.0
1.05	0.908	1.099	17.9	20.2
1.62	0.885	1.118	19.4	21.5
2.37	0.864	1.138	20.8	22.8
3.18	0.848	1.155	21.7	23.6
4.03	0.830	1.167	22.8	24.6
4.97	0.818	1.181	23.5	25.3
6.05	0.806	1.187	24.2	25.9
6.40	0.801	1.189	24.4	26.2
7.23	0.793	1.193	24.9	26.6
7.67	0.788	1.198	25.2	26.9

low symmetry structures are degenerate. This rules out electron-phonon coupling as the origin of the observed phase transition at $T_c = 370 \text{ K}$. To model electron correlations on Ti d orbitals we use the LDA+U approach, which requires the input parameters U and J . We propose to determine these parameters by calculating electron correlations on the TiF_6^{2-} ion and find $U = 8.1 \text{ eV}$ and $J = 0.9 \text{ eV}$. LDA+U predicts TiF_3 to be an antiferromagnetic insulator with spin $1/2$ per Ti. We find a long range order of Ti a_g orbitals with a wavevector (000) . The low temperature phase is lower in energy by about 900 K per TiF_3 in LDA+U calculations, which suggests electron-electron correlations to be present in this phase transition.

We explain the anomalously large higher order corrections in the Birch-Murnaghan fit and the observed volume at ambient pressure volume which is larger by 12% than the present theoretical prediction by two effects: (1) the presence of domain walls in the low symmetry phase and (2) the phonon contribution to the free energy. Using the experimentally determined c/a and V/V_0 ratios we find a global minimum at 14% (LDA) and 12% (LDA+U) volumes smaller than the observed ambient pressure volume. The experimental observations and theoretical calculations can be reconciled once domains are taken into account which stabilize the local minimum observed at ambient pressure. Under pressure this domain structure is altered and the volume is reduced to less than the global minimum once the crystal becomes a single domain and follows a compressibility behavior according to Eq. 6. In addition phonon contribution to the free energy, which is in principle pressure dependent, would alter the position of the global minimum and the bulk modulus. The Gruneisen parameter

calculations and experimental studies of the phonon spectrum under pressure will help to answer the question of relative importance of these contributions.

Acknowledgments

We are grateful to Fabian Essler for many valuable discussions, Warren Pickett for help in LDA+U calcu-

lations, and Dick Watson for useful suggestions. The computations were performed on the BNL galaxy cluster. This work was supported in part by DOE Grant No. DE-AC-02-98CH10886.

[1] A. Mogus-Milankovic, J. Ravez, J. P. Chaminade, and P. Hagenmuller, *Materials Res. Bulletin* **20**, 9 (1985).

[2] B. J. Kennedy and T. Vogt, *Materials Res. Bulletin* **37**, 77 (2002).

[3] J. Ravez, A. Mogus-Milankovic, J. P. Chaminade, *Mater. Res. Bull.* **20**, 9 (1985).

[4] P. Daniel, A. Bulou, M. Rousseau, J. L. Fourquet, J. Nouet, M. Leblanc, and R. Burriel, *J. Phys. Cond. Matt.* **2**, 5663 (1990); P. Daniel, A. Bulou, M. Rousseau, J. Nouet, and M. Leblanc, *Phys. Rev. B* **42**, 10545 (1990).

[5] Y. R. Chen, V. Perebeinos, P. B. Allen

[6] V. I. Anisimov and O. Gunnarsson, *Phys. Rev. B* **43**, 7570 (1991); V. I. Anisimov, J. Zaanen, and O. K. Andersen, *Phys. Rev. B* **44**, 943 (1991).

[7] W. E. Pickett, S. C. Erwin, and E. C. Ethridge, *Phys. Rev. B* **58**, 1201 (1998).

[8] S. Satpathy, Z. S. Popovic, and F. R. Vukajlovic, *Phys. Rev. Lett.* **76**, 960 (1996).

[9] M. R. Pederson and K. A. Jackson, *Phys. Rev. B* **41**, 7453 (1990); K. A. Jackson and M. R. Pederson, *Phys. Rev. B* **42**, 3276 (1990); M. R. Pederson and K. A. Jackson, *Phys. Rev. B* **43**, 7312 (1991); D. V. Porezag and M. R. Pederson, *Phys. Rev. B* **54**, 7830 (1996); A. Briley, M. R. Pederson, K. A. Jackson, D. C. Patton, and D. V. Porezag, *Phys. Rev. B* **58**, 1786 (1998).

[10] D. J. Singh, *Planewaves, Pseudopotentials and the LAPW Method* (Kluwer Academic, Boston, 1994).

[11] D. J. Singh, *Phys. rev. B* **43**, 6388 (1991).

[12] P. Blaha, K. Schwarz, and J. Luitz, in *Proceedings of WIEN97* (Techn. Universität Wien, Austria, 1999).

[13] J. P. Perdew and Y. Wang, *Phys. Rev. B* **45**, 13244 (1992).

[14] F. D. Murnaghan, *Am. J. Math.*, **49**, 235 (1937).

[15] V. I. Anisimov, I. V. Solovyev, M. A. Korotin, M. T. Czyzyk, and G. A. Sawatzky, *Phys. Rev. B* **48**, 16929 (1993); I. V. Solovyev, P. H. Dederichs, and V. I. Anisimov, *Phys. Rev. B* **50** 16861 (1994); A. I. Liechtenstein, V. I. Anisimov, and J. Zaanen, *Phys. Rev. B* **52**, 5467 (1995); A. B. Shick, A. I. Liechtenstein, and W. E. Pickett, *Phys. Rev. B* **60**, 10763 (1999).

[16] J. C. Slater and G. F. Koster, *Phys. Rev.* **94**, 1498 (1954).

[17] P. H. Dederichs, S. Blügel, R. Zeller, and H. Ahai, *Phys. Rev. Lett.* **53**, 2512 (1984).

[18] H. Sawada and K. Terakura, *Phys. Rev. B* **58**, 6831 (1998).

[19] Y. Okimoto, T. Katsufuji, Y. Okada, T. Arima, and Y. Tokura, *Phys. Rev. B* **51**, 9581 (1995).

[20] P. W. Anderson, *Phys. Rev.* **86**, 694 (1952).

[21] A. W. Sandvik, *Phys. Rev. Lett.* **80**, 5196 (1998).

[22] T. Vogt et. al., unpublished.

[23] H. Sowa and H. Ahsbahs, *Acta Cryst. B* **54**, 578 (1998).